

Efficient Tabular Data Preprocessing of ML Pipelines

Yu Zhu
Systems Group, Department of
Computer Science
ETH Zurich, Switzerland
yu.zhu@inf.ethz.ch

Wenqi Jiang
Systems Group, Department of
Computer Science
ETH Zurich, Switzerland
wenqi.jiang@inf.ethz.ch

Gustavo Alonso
Systems Group, Department of
Computer Science
ETH Zurich, Switzerland
alonso@inf.ethz.ch

ABSTRACT

Data preprocessing pipelines, which includes data decoding, cleaning, and transforming, are a crucial component of Machine Learning (ML) training. They are computationally intensive and often become a major bottleneck, due to the increasing performance gap between the CPUs used for preprocessing and the GPUs used for model training. Recent studies show that a significant number of CPUs across several machines are required to achieve sufficient throughput to saturate the GPUs, leading to increased resource and energy consumption. When the pipeline involves vocabulary generation, the preprocessing performance scales poorly due to significant row-wise synchronization overhead between different CPU cores and servers. To address this limitation, in this paper we present the design of PIPER, a hardware accelerator for tabular data preprocessing, prototype it on FPGAs, and demonstrate its potential for training pipelines of commercial recommender systems. PIPER achieves 4.7 ~ 71.3 \times speedup in latency over a 128-core CPU server and outperforms a data-center GPU by 4.8~ 20.3 \times when using binary input. The impressive performance showcases PIPER’s potential to increase the efficiency of data preprocessing pipelines and significantly reduce their resource consumption.

1 INTRODUCTION

Data preprocessing is a critical step in machine learning (ML) training systems, significantly influencing the quality of the resulting models. It aims to improve model accuracy and involves several key steps, such as data normalization, handling missing values, feature encoding, or data augmentation. Current ML training systems employ a hybrid CPU-GPU architecture [79], where the CPU handles data preprocessing before the data is transferred to the GPU for training, (upper part of Figure 2).

GPU performance has seen rapid advancements in recent years [15], while CPU performance improvements have lagged behind. As a result, data preprocessing is often a bottleneck in ML training systems due to the increasing performance gap between CPUs and GPUs, as recently discussed in commercial cloud deployments [81, 82]. To accelerate preprocessing on CPUs, frameworks such as *tf.data* [52] are employed, combined with various distributed and parallel processing techniques to improve throughput [6, 23, 81, 82]. A common approach is to use several machines to process the data needed to feed a GPU [82] which provides the required performance but it implies a huge increase in the resources needed and negatively impacts the overall efficiency and cost of the system. But even ignoring the issues of resource and energy inefficiency, a significant challenge remains: *how to efficiently handle stateful operators in the preprocessing pipeline?* The costly synchronizations of internal states across many CPU cores and servers often negate the benefits

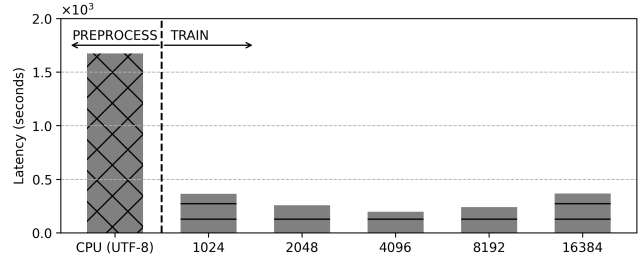


Figure 1: Preprocessing vs training (one epoch, different batch sizes on one GPU).

of adding additional CPU resources [16, 20, 31, 32], presenting a challenge that is difficult to handle at the software level and cannot be solved by simply adding more CPU cores.

We have conducted a number of initial experiments to understand the gap between the CPU and the GPU. We have trained a model similar to that used by Meta [82] with various batch sizes in Google Cloud (12 vCPUs, 64GB RAM, 16GB Nvidia V100 GPU). In Figure 1 we show the result of comparing the time it takes to train one epoch on the GPU for different batch sizes and the time it takes for the corresponding data preprocessing pipeline. The first observation is that we measure a maximum GPU Utilization of 40%, clearly indicating that the GPU is being infrautilized. The bottleneck is clearly visible in Figure 1 when comparing the time the CPU needs to process the input and the time if taking the GPU to train. Even when using large batches, the training is significantly faster than the input preprocessing.

These results confirm those reported in by Meta [82] and motivate us to try to accelerate the preprocessing stage with the goal of increasing the overall efficiency of the system. To this end, in this paper we propose PIPER, a network-attached accelerator for efficient stateful data preprocessing (Figure 2). PIPER achieves high-performance and scalable data preprocessing through several novel ideas. First, PIPER avoids costly explicit synchronization. PIPER adopts a column-wise pipelined execution mechanism, and the heterogeneous hardware processing elements operate on different feature columns independently. Second, PIPER achieves high memory bandwidth by utilizing not only on-chip SRAM but also fast off-chip High-Bandwidth Memory (HBM). Third, we propose a novel parallel decoding mechanism and implement it on PIPER, such that the accelerator efficiently decodes raw datasets. Finally, PIPER can be directly attached to the network, such that (a) it can be easily integrated into existing ML training systems without the need to install FPGAs on training servers; (b) the FPGA is capable

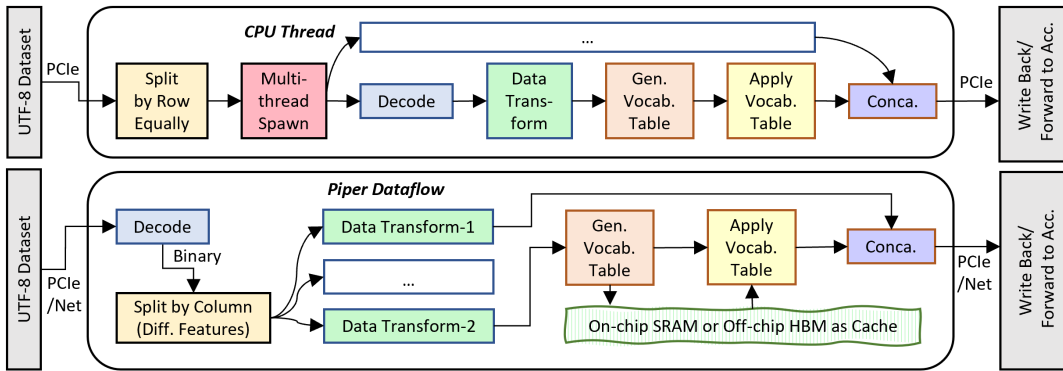


Figure 2: System overview for DLRM data preprocessing pipeline on CPUs and PIPER, respectively. PIPER supports both PCIe and the network as the data movement interface. The white blocks represent parallel workers.

of processing datasets larger than its memory capacity in a streaming fashion; and (c) the number of preprocessing accelerators and training accelerators can be scaled independently.

We choose FPGAs as the hardware platform to prototype PIPER since FPGAs are widely available from major cloud vendors, including AWS [3], Microsoft Azure [21, 64], and Alibaba Cloud [45, 80], facilitating the deployment of PIPER in data centers. Moreover, FPGAs offer greater architectural flexibility as, e.g., they can be used as smart NICs on training servers, loading raw data from the network and feeding the preprocessed data directly to GPUs [75].

We have evaluated PIPER on production Deep Learning Recommender Models (DLRMs) from Meta and Google [26, 53]. PIPER outperforms a 128-core CPU server, achieving speedups between 4.7~71.3 \times across various configurations. When processing the raw encoded datasets, PIPER attains 5.1 \times and 4.7 \times speedup over the CPU when using on-chip SRAM and off-chip HBM, respectively. With decoded binary datasets as input, the performance gains with PIPER rise to 71.3 \times and 25.7 \times when using on-chip and off-chip memory. Compared to a GPU, especially dealing with binary format, PIPER provides speedups ranging from 4.8 \times to 20.3 \times .

PIPER makes the following contributions:

- We measure the performance of embedding generations during the overall ML training process, and analyze both CPU-optimized and GPU-accelerated solutions to establish a baseline for tabular data preprocessing.
- We describe the design of PIPER, a hardware accelerator targeting stateful preprocessing data pipelines for ML that includes efficient novel data decoding units and specialized hardware units for various operators.
- We integrate PIPER with a hardware network stack, facilitating its flexible and scalable deployments.
- We evaluate PIPER on production Deep Learning Recommendation Models (DLRMs), representative ML models for recommender systems, showing that it can be used across different datasets and demonstrating its advantages over powerful server-level CPUs and GPUs.

2 BACKGROUND AND MOTIVATION

Data preprocessing pipelines are fundamental for ensuring model quality in ML systems. Such pipelines process raw data through

multiple stages to transform it into a refined format suitable for model training. Preprocessing tasks include, e.g., decoding, transforming different data types, normalization, and format conversions, which are crucial for capturing critical information.

2.1 Preprocessing for Tabular Dataset

The input format for ML training varies for different applications, including tabular data, audio/images/videos, texts, graphs, etc. The processing for tabular data often involves embedding generation, an efficient feature representation method, referring to the technique to represent high-dimensional, categorical, or structured data in a low-dimensional, continuous vector space, which helps capture the relationships and similarities among data points in the embedding space. Various ML tasks have integrate embedding to help improve the model performance, for example, NLP-related models (RNNs [49], LSTMs [24], BERT [17], GPT [1]) rely on embeddings to represent words or tokens as dense vectors to feed into the input layer. Pre-trained word embeddings with limited vocabulary size, such as Word2Vec [13], GloVe [62], are popular and help developers directly map their texts into the corresponding embeddings and initialize training easily.

For ML-based recommender systems, such as DLRM [26], Wide and Deep [11], Neural Collaborative Filtering [29], Variational Autoencoder [37], BERT4REC [68], the scenario is a bit different. These ML-based models share a similar data input format and embedding is a common technique to help transform non-trainable parameters into learnable representations. The difference from NLP-based models lies in the non-unified embedding space, e.g., for attributes such as User-ID which leads to sparse embeddings requiring a much larger space to explore and is highly application dependent. In such conditions, use cases in social or streaming media need to maintain tailored embedding spaces for independent training of models.

2.2 Deep Learning Recommender Models

DLRMs, widely used in recommender systems, are popular machine learning models that provide content recommendations based on the user’s personal preferences. They are used in many areas, ranging from e-commerce [85], content streaming [84], as well as online advertising [25].

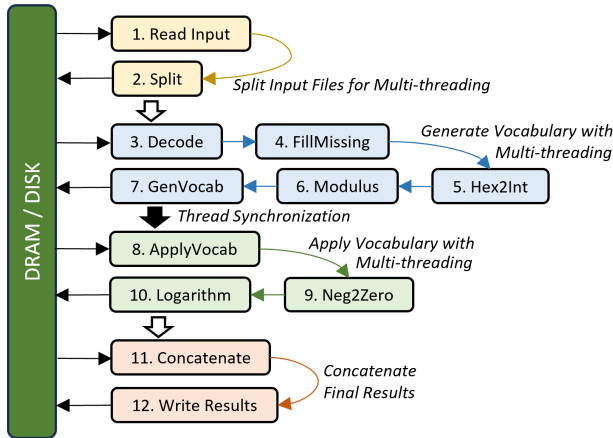


Figure 3: Dataflow of preprocessing pipelines in CPU.

Recommender systems mainly rely on two primary categories of features: *dense features* and *sparse features*. Dense features are predominantly non-zero or complete. Examples of attributes that lead to dense features are user age, item pricing, or a movie’s average rating. These features, often numerical, are generally normalized to ensure zero mean and unit variance or adjusted to fit a specific range, which helps ML algorithms converge. Sparse features, typically categorical, are those with predominantly zero or absent values because they capture a domain not easily represented in a linear scale. For instance, features turn sparse when a vast dataset is one-hot encoded for user IDs or when textual content gets described as a bag of words. These features are then turned into binary vectors through embedding. ML-based recommender systems need to handle both dense and sparse features, which poses a design challenge. Most of the work done on the data preprocessing pipelines involves generating the proper embeddings and data representations for the raw training data.

2.3 CPU-based Preprocessing Pipelines

In this paper, we use two representative examples from Meta [50] and Google [71] to illustrate the preprocessing stages used in practice and run on CPUs. Table 1 lists the detailed functionalities of the involved operators. Among them, *GenVocab* is responsible to create a vocabulary table for all columns of sparse features, and *ApplyVocab* then iterates anew over the dataset to generate the final embedding table.

Meta’s DLRM pipeline. Meta [50] released an open-source DLRM project as a benchmark for personalized recommendation models (Figure 3). Aside from some common transformation operators, like *modulus*, *logarithm*, one particular step, the generation of vocabulary table, makes the pipeline *stateful* and introduces extra overhead for synchronization when employing multi-threading. After retrieving data from the disk, the CPU sequentially processes the dataflow and writes the computed results back into memory or storage. The input data format is typically encoded in UTF-8, consisting of both sparse and dense features. To make it easier to understand the pipeline and the rest of the design we propose, we divide the process into four well-separated stages: *Split Input File*, *Generate Vocabulary*, *Apply Vocabulary* & *Concatenate Final*

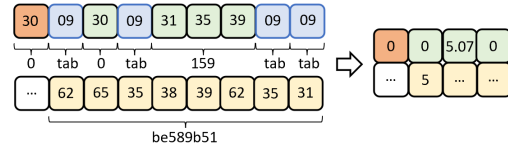


Figure 4: An example of data preprocessing for a row of raw UTF-8 data, in which orange represents the labels, blue denotes tabs, green indicates dense features, and yellow denotes sparse features (8-byte hash values).

Results (we merge some other data transformations into *Generate Vocabulary* & *Apply Vocabulary* for simplicity). Figure 4 shows an example of the inputs and outputs of the data preprocessing. The input file is encoded using UTF-8 with ASCII characters, while the output consists of the transformed features.

Split Input File (SIF). This step involves (1) reading the entire dataset from storage, counting the number of rows, and (2) partitioning the input equally as intermediate sub-files. The number of sub-files corresponds to the pre-defined number of threads.

Generate Vocabulary (GV). This step deals with the first part of processing individual sub-files and constructs embedding tables for the sparse features. The program processes sub-files in parallel using multiple threads. (3 & 4) Each thread reads intermediate sub-files created during the SIF step and decodes the UTF-8 data into 32-bit width. The delimiter of the original dataset is `\t`, with default value 0 for empty entries, irrespective of whether the feature is sparse or dense. (5) Original sparse features are hashed into hexadecimal values for security reasons. Thus, each thread has to convert them first to decimal values before processing. (6) A positive modulus operation sets the range of sparse features to limit the size and determine the dimensionality of the embedding table. (7) Each thread creates a sub-dictionary to collect the appearing sequence for each unique sparse feature and stores the partially processed data during the GV step into the disk for the following operations. The program then synchronizes the threads and combines these sub-dictionaries for a unified embedding table.

Apply Vocabulary (AV). This step starts after generating the full vocabulary table, and the partially processed data from GV serves as input. Enabling multi-threading can also expedite this process. (8) Each thread maps sparse features to their corresponding values in the shared vocabulary table. (9) Each thread sets negative values of dense features as zero due to non-negativity constraints. (10) Logarithm operation of dense features is optional, contributing to reducing skewness and scaling down large values. Each thread then saves intermediate results to memory or disk.

Concatenate Final Results (CFR). (11 & 12) In the final step, merging multiple intermediate results and consolidating them into a single file is necessary as ML models require complete rows as the input. The default algorithm is the simple concatenation operation in sequence.

Google’s DLRM pipeline. Google [71] open-sourced another DLRM project, where the pipeline is similar and Table 1 covers all operators in both pipelines. An advantage of Google’s solution for preprocessing is its integration in Apache Beam, making it easier to use in cloud environments.

Table 1: Preprocessing transformations available.

Op Name	Description
Decode	Decode UTF-8 dataset for processing
FillMissing	Fill missing values for all features
Hex2Int	Convert hexadecimal values to decimal (sparse)
Modulus	Compute positive modulus (sparse)
GenVocab	Extract a set of unique IDs (sparse)
ApplyVocab	Generate integer-encoded mappings (sparse)
Neg2Zero	Change negative values to zero (dense)
Logarithm	Do $\log(x+1)$ operation (dense)
Concatenate	Concatenate final results from multiple threads

2.4 Inefficiencies in CPU-based Data Preprocessing

As reported by Meta [82], data preprocessing is a major bottleneck in production DLRM systems, leading to significant GPUs underutilization. Meta uses the DSI (Data Storage & Ingestion) pipeline to produce data for training, which consists of *offline data generation*, *dataset storage*, and *online preprocessing services*. Such pipeline is conceptually similar to that used in databases for Extract, Transform, and Load (ETL) operations [46, 65, 69, 78]. In the context of DLRMs, the large scale of the models involved, the need to frequently update them, and the fast-evolving features of the model result in a massive amount of data that has to be preprocessed and fed to the domain-specific accelerators. In their experiments, they run a training job as the baseline on a two-socket, 28-core CPU machine for preprocessing, two 100 Gbps NICs for data ingestion, and 8 Nvidia V100 GPUs for training. They observe that almost 56% of the GPU cycles are wasted while waiting for training data despite the CPUs operating at 92% utilization. Alibaba [81] has also reported similar inefficiencies in their data centers as a result of the CPU-GPU performance mismatch. Given the growth in dataset sizes and the need to retrain models on a regular basis, the CPU bottleneck will become even more prominent, especially considering that the performance of GPUs is evolving much faster than that of CPUs [12].

Meta addresses the GPU resource underutilization problem by disaggregating and scaling out the data preprocessing tasks across many servers [82]. However, this scale-out strategy is not efficient for two reasons. First, while the performance improves by using more CPU servers, it also results in a much higher resource and energy consumption. Second, the performance of stateful row-based multi-processing does not scale linearly with the amount of CPU resources, as we will show in the experiments. This is due to the high synchronization overheads between the CPU threads of different processing stages: after each thread processes rows of data, a costly synchronization step must be used to exchange internal states to form the unified embedding table for single column.

Choice of multi-processing. The default data partitioning method in CPU-based preprocessing pipelines typically divides the dataset into chunks of rows, with each thread handling a portion of these rows using the same operations. This row-wise processing approach supports varying numbers of CPU threads and aligns well with the row-wise input format commonly required for machine learning training. However, it comes with the downside of necessary synchronization overhead, which can affect performance.

Alternatively, column-wise multiprocessing assigns each thread to handle independent columns, which can reduce the execution time for processing each column. This method is advantageous for tasks where column-level operations dominate. However, a key limitation is that the number of CPU threads must match the number of columns, which can be restrictive. Another disadvantage is the unbalanced workload for different columns. Additionally, since most ML models require row-wise input, column-wise processing necessitates the concatenation of all columns back into rows, potentially leading to I/O bottlenecks. The choice between these two multiprocessing methods depends on several factors, including the hardware platform, the structure of the dataset, and the specific requirements of the processing pipeline.

2.5 GPU-based Data Preprocessing

GPU-accelerated preprocessing is an appealing approach to avoid having to move the data from the CPU to the GPU. For instance, Nvidia’s Data Loading Library (DALI) [55] is used for image preprocessing. The acceleration for recommender systems in GPU is also possible based on Nvidia RAPIDS suite [56–58].

The acceleration of GPU also benefits from column-wise processing. For example, Parquet [74], a popular columnar storage file format, allows GPU to process columns independently among Streaming Multiprocessors (SMs) and maximize row-level parallelism by CUDA cores within an SM. This method is a combination of row-wise and column-wise multi-processing. We will compare our design against these methods in the experimental analysis.

3 PIPER: ACCELERATED DATA PREPROCESSING

We present PIPER, a pure column-wise high-performance accelerator for tabular data preprocessing pipelines. We propose multiple techniques to optimize accelerator performance, including transforming raw datasets in parallel, broadcast-gather processing element (PE) design, high-bandwidth memory (HBM) as a cache, and reducing data movement via a direct network interface. Other intrinsic factors contributing to the high performance of PIPER involve pipelined processing and low synchronization overhead.

3.1 Accelerator Overview

Accelerator components. Figure 5 shows the accelerator overview of PIPER. The accelerator consists of various specialized hardware Processing Elements (PEs), including *LoadData*, *Decode*, *Neg2Zero*, *Logarithm*, *Hex2Int*, *Modulus*, *GenVocab*, *ApplyVocab* & *StoreData*. The performance of each processing stage can be controlled via instantiating multiple PEs. The accelerator can work as either a local accelerator, loading data from and storing results to local DRAM, or as a network-attached accelerator using the FPGA TCP/IP stack.

Processing control flow. Figure 5 shows the dataflow with the operators in the FPGA and the slight adjustment of the original sequence of operators, as we can merge some of them to simplify the overall dataflow. Once the dataset is decoded, the data preprocessing is conducted via two consecutive loops. In the first loop, PIPER reads the whole dataset and generates the corresponding vocabulary table. The size of vocabulary determines whether it is stored in on-chip SRAM or off-chip HBM, which significantly influences

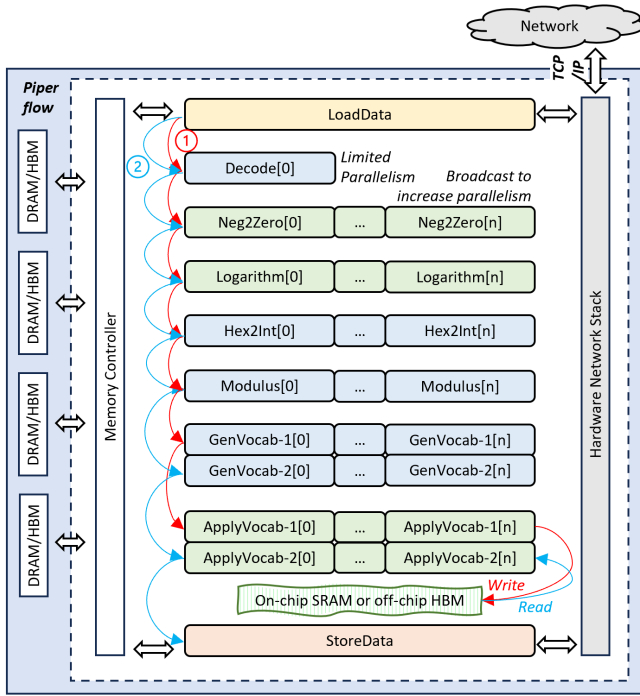


Figure 5: PIPER accelerator overview. The dataflow involves two consecutive loops ① & ②. We use the same color of blocks as in Figure 3 to represent different types of operators.

the overall performance due to random memory accesses. In the second loop, PIPER rereads the dataset and maps each feature into the corresponding value in the vocabulary table. *GenVocab* and *ApplyVocab* behave differently in the 1st and 2nd loops, while other PEs behave the same to process input features. For *GenVocab*, it filters some unique inputs in the first loop and passes all inputs in the second loop. For *ApplyVocab*, it writes the appearing sequence of unique inputs into memory in the first loop and reads corresponding values in the second loop. Some operators listed in Table 1 are missing in Figure 5, like *FillMissing* & *Hex2Int*, because the FPGA handles bits directly and there is no need for representing *Null* as in software, so the default value for the empty element after *Decode* is 0, and there is no need to transform from hexadecimal to decimal explicitly. Each PE is a computing unit on the FPGA, and different PEs are interconnected via FIFO channels.

Differences between CPU and PIPER. In multi-threaded CPU implementations, the dataset is partitioned by rows. Each thread handles a small portion of the entire dataset, and synchronization is required once all threads have completed their tasks, as shown in Figure 3. In contrast, the FPGA is a spatial dataflow processor with heterogeneous hardware processing elements (PEs) that can process columns of data in parallel. Instead of partitioning data by rows, an FPGA can efficiently process raw data in a column-wise fashion. Here a dataflow in FPGA corresponds to the concept of SM in GPU. This is because the heterogeneous hardware PEs are specialized for processing each feature column, allowing them to handle different columns with consistent throughput. Besides, the output of processing different features in one FPGA can aggregate

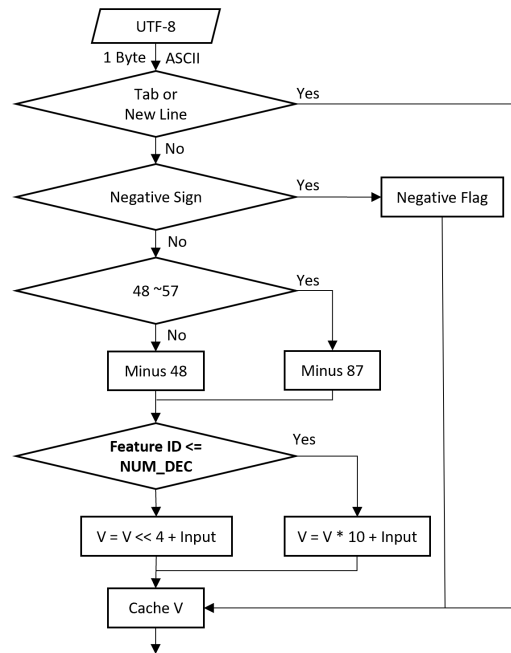


Figure 6: Flow chart to decode UTF-8.

together easily, which helps store the processed dataset in the row-wise manner. This is not easy on the CPU due to the homogeneous nature of CPU cores. Thus, compared to CPUs, the FPGA not only includes specialized high-performance PEs but also eliminates the need for synchronization required in CPU-based solutions.

3.2 High-Performance Processing Elements

We now introduce the high-performance Processing Elements (PEs) instantiated on PIPER in detail.

LoadData. This PE aims to load the dataset from either FPGA’s off-chip memory or the network. If the data is loaded from the memory, the bandwidth is determined by the width of the memory interface and the number of memory channels. The achieved *Initialization Interval (II)*, which defines the minimum number of clock cycles required between successive launches of operations in a pipelined design, is as low as one clock cycle.

Decode. This PE aims to decode the input UTF-8 data and convert them to various features used for the model, and is one of the accelerator’s bottlenecks that we will discuss later. Figure 6 shows a rough dataflow of implementing *Decode* in FPGA. The valid input memory port width is one byte, and the achieved II is one cycle. For the dataset of DLRM, five kinds of ASCII values are possible: *horizontal tab* \t, *new line* \n, *minus sign* -, 0~9 and a~f. PIPER use \t and \n as delimiters: \t to split features and \n to denote the end of the row. It creates a boolean value *negative_flag* to represent *minus sign* and decode ASCII values of 0~f to corresponding hexadecimal bits. Then, it keeps track of the input character in a 32-bit register to transform the combination of characters 0 ~ f to expected values. (a) For dense features (decimal values), it multiplies with ten and add the current input. Due to the existence of negative values, it keeps the *negative_flag* to denote whether the current value should be negative or not and regard the following binary characters as

positive in the register. (b) For sparse features (hexadecimal values), it shifts the cached register 4 bits left every cycle and add the current input. Sparse features are always positive, and it omits *negative_flag* for them. (c) When reaching delimiters $\backslash t$ or $\backslash n$, it extracts the current value in the register. If *negative_flag* is true, it transforms the value to the corresponding *two's complement*; otherwise, it outputs the value directly. It transfer the final output to downstream modules and reset the register to zero for the subsequent decoding. Figure 6 presents the flow chart of decoding UTF-8 in FPGA. This is a common solution, as it can explicitly separate the processing of decimal and hexadecimal values, and what we should know in advance is the data format for each feature.

Neg2Zero. This is a ternary operator. It sets the negative input dense feature to 0, otherwise it keeps the original value as output. The achieved II is one cycle.

Logarithm. We calculate the logarithm using the default operator. The achieved II is one cycle.

Modulus. We use the modulus operator to limit the range of sparse features. The achieved II is one cycle.

GenVocab-1. This PE aims to extract unique values for inputs. We keep a bitmap in BRAM/URAM and pass unique inputs to downstream modules. The achieved II is two cycles.

GenVocab-2. We pass inputs to downstream modules directly. The achieved II is two cycles because the performance is limited by the PEs for *GenVocab-1*.

ApplyVocab-1. This PE aims to count the appearing sequence for unique inputs from upstream modules. We keep a counter and write the current counter value into the corresponding position in the vocabulary table. The achieved II is two cycles for a small vocabulary table in on-chip RAM and is about 15 cycles for a large vocabulary table in off-chip HBM due to random memory write.

ApplyVocab-2. This PE aims to assign values to all sparse features. We fetch the corresponding value from the vocabulary table for each input feature. The achieved II is two cycles for a small vocabulary table in on-chip RAM and is about 15 cycles for a large vocabulary table due to random memory read.

StoreData. We combine the results from different dataflows and write them back to FPGA's off-chip memory or to the network. The achieved II is one cycle.

We implement all aforementioned operators in the high-level modular design which allows the easy connection in the pipeline and potentially add/remove/change some operators to meet the new requirement.

3.3 Efficient Raw Dataset Transformation

Data format transformation from UTF-8 to binary, like Parquet [74] or TFRecord [22], is not free, no matter in CPU or in GPU. A straightforward implementation of the *Decode* PE in FPGA would become the system bottleneck and result in low accelerator performance. The memory interface width on FPGA is up to 512 bits, which retrieves 64 bytes of data per cycle. As FPGA runs different modules in the pipeline, the operator with the largest II determines the performance of the entire dataflow. The achieved II for a simple *Decode* PE in FPGA is one cycle, but the effective throughput is very low as *Decode* can only process one byte per cycle. The theoretical throughput of one DDR channel is 19GB/s (512-bit wide

memory lane, 300MHz), but decoding data per byte is 64 times slower and limits the valid throughput to 300MB/s. Each row of the input UTF-8 encoded data comprises hundreds of bytes and *PIPEP* takes the same number of cycles to read them. During this process, downstream operations for both sparse and dense features must wait and can not run in parallel because they compete for the input.

To mitigate this bottleneck, we propose a high-performance parallel UTF-8 decoding unit to improve the overall throughput of the accelerator. Here, we make some assumptions for the simplified description. Firstly, we regard $\backslash t$ and $\backslash n$ the same as they both serve as delimiters. Secondly, we ignore the *minus sign* because it only requires to create a *negative_flag* to represent the sign of decimal values and calculate the *two's complement* for output. Thirdly, we only consider the condition for hexadecimal values because we can transform from hexadecimal values to the original integers easily. Finally, we split the decoding process into multiple modules to make the entire structure more straightforward: (a) the upstream module serves to map ASCII values to $\backslash t$, $\backslash n$, - and $0\sim f$; (b) the downstream module is a state machine that extracts valid 32-bit outputs from the 128-bit wide input stream (the number of valid outputs ranges from 0 to 4).

```

0b1111: o0 = v; o1 = 0; o2 = 0; o3 = 0; v = 0;

0b1110: o0 = v; o1 = 0; o2 = 0; v = s3;
0b1101: o0 = v; o1 = 0; o2 = s2; v = 0;
0b1011: o0 = v; o1 = s1; o2 = 0; v = 0;
0b0111: o0 = v << 4 + s0; o1 = 0; o2 = 0; v = 0;

0b1100: o0 = v; o1 = 0; v = s2 << 4 + s3;
0b1010: o0 = v; o1 = s1; v = s3;
0b1001: o0 = v; o1 = s2 << 4 + s3; v = 0;
0b0110: o0 = v << 4 + s0; o1 = 0; v = s3;
0b0101: o0 = v << 4 + s0; o1 = s2; v = 0;
0b0011: o0 = v << 8 + s0 << 4 + s1; o2 = 0; v = 0;

0b1000: o0 = 0; v = s1 << 8 + s2 << 4 + s3;
0b0100: o0 = v << 4 + s0; v = s2 << 4 + s3;
0b0010: o0 = v << 8 + s0 << 4 + s1; v = s3;
0b0001: o0 = v << 12 + s0 << 8 + s1 << 4 + s2; v = 0;

0b0000: v = v << 16 + s0 << 12 + s1 << 8 + s2 << 4 + s3;

```

Script 1: Parallel decoding for UTF-8

Script 1 shows the parallel decoding process. The module's input is four bytes, and we split them into 4×8 -bit sub-inputs as s_0 , s_1 , s_2 & s_3 . We store the cached value in the register as v . We set four possible outputs as o_0 , o_1 , o_2 & o_3 . First, we count how many $\backslash t$ exist in the input because it determines the number of valid outputs. There are in total 16 combinations: four outputs ($0b1111$), three outputs ($0b1110$, 1101 , 1011 , 0111), two outputs ($0b1100$, 1010 , 1001 , 0110 , 0101 , 0011), one output ($0b1000$, 0100 , 0010 , 0001) and no output ($0b0000$), as shown in Script 1. We use the four-byte version in the final design to increase the efficiency of *Decode*, and in this case, *GenVocab* becomes the bottleneck which runs slower due to the requirement of updating in two cycles for each feature. Decoding eight bytes or higher in parallel is also feasible, which would contain 256 combinations or we can assemble it from two four-byte versions.

Besides, dataset compression/decompression is a popular topic for hardware accelerator [8, 44, 59, 66]. For example, converting storage-focused file formats Apache Parquet to in-memory data

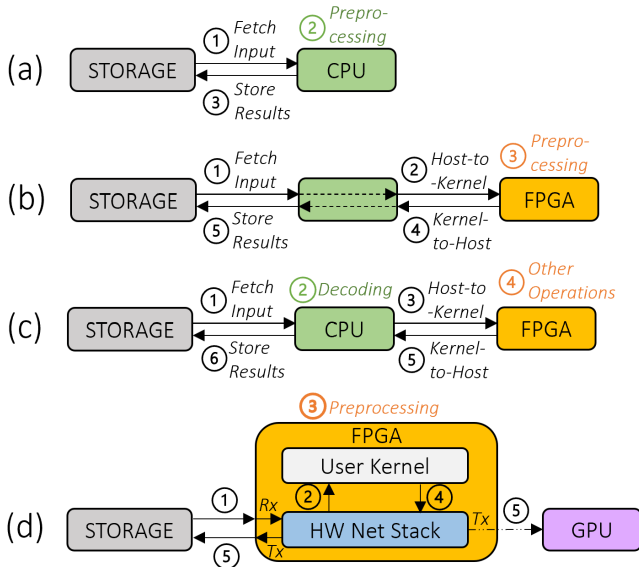


Figure 7: Data movements and processing patterns. Traditional: (a). Ours: (b), (c), (d).

structures Apache Arrow has drawn the attention of FPGA community [59, 60], which helps generate the output in line-rate. In this paper, we omit the discussion of compressing binary file or not.

3.4 System Integration

Figure 7 presents four different communication patterns between CPU and FPGA to conduct data preprocessing. Figure 7a shows the architecture of the conventional CPU-based preprocessing pipeline. Figure 7b displays the conventional way of offloading all operations into FPGA, which serves as a complementary accelerator to CPUs. CPU is responsible for data loading, first storing data in its buffer and transferring it to FPGA’s off-chip memory via the PCIe channel. Figure 7c illustrates that we can enable co-processing between CPU and FPGA for higher performance. Now, we partition the pipeline into two parts, finishing the data decoding in CPU and transferring decoded data to FPGA to finish the rest of the operations. Figure 7d shows the network-based solution of PIPER for online preprocessing where the host-side logic is removed and final results are transferred to ML accelerators for further training/inference directly. This network-based configuration not only improves end-to-end preprocessing performance by eliminating host-side overhead but also enables streaming data processing, supporting datasets larger than the FPGA’s memory capacity.

3.4.1 PIPER as a Local Accelerator. The execution of PIPER in the local environment shows the effectiveness of offloading preprocessing tasks into FPGA. However, it also exposes some shortcomings compared to the network-attached mode, as we will explain below.

Kernel launching procedure. Figure 7b shows how we start by offloading all operations to the FPGA as a PCIe-attached accelerator, initiating with the decoding of UTF-8 data. As described earlier, FPGAs cannot read data directly from the disk. Following the common procedure, we create a buffer on the host server, load data into this

buffer, and transfer it to the corresponding off-chip memory channels of the FPGA. The disadvantage of this architecture is that the buffer-related operations are costly, as we will present in Section 4. This is because such a communication pattern is that all these stages must execute in sequence, and there is no overlap among them to help increase throughput. Besides, as *Decode* cannot fully utilize all memory channels, the dataflow processes one feature at a time rather than processing the entire row. The valid width of streams between modules is limited to 32-bit.

Relocate decoding to CPU. Figure 7c illustrates the communication pattern for the co-processing between the host (CPU) and the kernel (FPGA). Offloading all operations into FPGA limits the degree of parallelism as we can at most handle one feature at a time due to the low throughput of *Decode*. An intriguing point of comparison arises when relocating the *Decode* function to the CPU and subsequently transferring the decoded data into FPGA’s off-chip memory for further processing. When making this comparison, we consistently consider the total execution time for both the host and the kernel. We achieve maximum parallelism by segregating sparse and dense features into separate memory channels, digesting 3×512 bits per cycle from DDR. Consequently, individual column processing emerges as the optimal choice, and FPGA benefits from this kind of column-based parallelism. Currently, one DDR channel reads the label key and dense features (1+13 integers, yielding 448 valid bits from one 512-bit wide memory lane and setting any invalid bits to 0), while two DDR channels handle sparse features (26 integers, producing 832/1024 valid bits from two memory lanes, also setting invalid bits to 0). This arrangement enables division into independent sub-tasks to handle each input feature in parallel. Leveraging FPGA’s streaming capabilities ensures seamless integration of results from all features, regardless of varying feature processing latency. When we put *Decode* function in the attached CPU, the overall dataflow in the kernel is the same as in Figure 5. The difference is that we can now increase the number of PEs to maximize parallelism.

Binary Input & Burst Read. Figure 7b and 7c displays the difference of executing *Decode* in the host or in the kernel, and one significant difference is the valid memory throughput limited by *Decode*. Here, we explore the potential of utilizing a binary dataset as the input because the overhead introduced by the decoding process is unnecessary when the content is binary. To highlight the positive effect, we do thorough experiments based on the pre-decoded binary dataset, followed by the same procedure in section 2.3. We maximize the performance with parallel dataflows, and the communication pattern is the same as Figure 7b, eliminating the need for an additional decoding operator. In Section 4, We test the performance of the CPU/GPU with binary input for a fair comparison, and we further demonstrate the inefficiency challenges posed by decoding UTF-8.

3.4.2 PIPER as a Network-attached Accelerator. Figure 7d presents a solution leveraging disaggregated storage and computation through a high-throughput network to overlap data movement with computing operation, inspired by previous work that disaggregate storage & compute [4, 38, 39, 41, 61, 86] and SmartNIC [2, 10, 19, 21, 30, 33, 43, 72, 75]. In this way, we integrate the data loading process into the whole dataflow, and now all steps run in a fully pipelined

method. In this setup, the datasets are sent to the target FPGA for preprocessing via the network. After data preprocessing, FPGA can send the results to CPUs, which can then either write them back to disk or forward them to other ML inference or training accelerators such as GPUs.

Advantages. Such a network-attached design offers several advantages over the local accelerator architecture in terms of flexibility. First, the network-attached design avoids the host-side processing, which involves expensive operations including allocating a large buffer and data movements between disks, CPUs, and FPGAs. Second, the FPGA can process large-than memory datasets in a streaming fashion, without the need of storing the entire dataset in the FPGA memory before the processing. Thirdly, the disaggregated architecture offers the flexibility scale the number of FPGAs (pre-processing) and GPUs (training) individually according to various performance requirements. Finally, with a simple network-based interface, PIPER can be integrated into future ML systems seamlessly for online data preprocessing.

4 EVALUATION

We evaluate PIPER to answer these questions:

- I. How much performance advantage can PIPER gain over multi-core CPUs and data-center GPUs? Can PIPER speed up all the operators in the pipeline? § 4.4.6
- II. Can PIPER gain extra performance by exposing the network interface? Can the performance meet the requirements for online training? § 4.4.5
- III. What are the pros and cons of using HBM as a cache and using binary datasets as input? § 4.4.3, 4.4.5
- IV. What are the implications of allocating *Decode* to host or kernel? What can we learn from the local execution time breakdown? § 4.4.4, 4.4.2

4.1 Experimental Setup

Dataset. We evaluate the data preprocessing on the Criteo Kaggle dataset [14], a well-known DLRM dataset containing online advertising data for seven days. Each row contains one label key, 13 dense features (such as the number of times a user clicks on an advertisement), and 26 sparse features (anonymous and hashed string values representing various categorical information about the ads, user, and context). The raw UTF-8 dataset is 11GB, and the decoded binary dataset is 8.2GB.

Software Configuration. For the Meta baseline, we make optimizations for their native data preprocessing module [50] as the baseline. We execute the Google pipeline based on their Apache Beam implementation [71] that is integrated within Google Cloud. For the GPU part, we rent NVidia 16GB V100 in Google Cloud. For PIPER, we use Vitis HLS 2022.1 to compile the bitstream.

Hardware. We evaluate Meta’s CPU baseline on a two-socket server with AMD EPYC 7V13 CPU (128 cores in total without hyper-threading) and 512 GB DRAM. We evaluate Google’s preprocessing pipeline using a Google Cloud instance (c2d-highcpu-32) with AMD EPYC 7B13 16-core (32 threads) and 64 GB DRAM. We run GPU experiments in Nvidia 16GB-HBM2 V100, attached with Intel Skylake N1 12 vCPUs and 64 GB DRAM. We use two different FPGAs for PIPER as local and network-attached accelerators, respectively,

due to memory capacity considerations: using PIPER as a local accelerator requires larger memory capacity to store input and output datasets, whereas the network-attached accelerator processes data in a streaming fashion without the need for large memory capacity. For PIPER as a local accelerator, we use Xilinx Alveo U250 that is equipped with 64GB DDR (4 memory channels, maximum throughput 77GB/s) and 54MB SRAM. The attached CPU is an Intel Xeon 16-core Processor (Cascadelake). For PIPER with the network interface, we use Xilinx Alveo U55c equipped with 16GB HBM (32 memory channels, maximum throughput 460GB/s) and 43MB SRAM. The attached CPU is an AMD EPYC 7302P 16-core Processor with 32 hyper-threads.

4.2 Optimized CPU Baseline

To report the best baseline performance, we have made several optimizations to mitigate some unnecessary overheads.

4.2.1 Optimizing Meta’s DLRM Preprocessing. We show the effect of step-by-step optimizations for the baseline, including removing I/O overhead for input and output datasets, caching intermediate states in memory, and using decoded binary input datasets. The I/O overhead is similar in all designs, CPU or FPGA, with the difference that the FPGA network version can process data at line rate without copying to memory, which gives it a significant advantage. Thus, in the evaluation we focus solely on the processing performance of both approaches. We use three versions of the baseline.

Config I. In this setup, we assume the input dataset is loaded from memory instead of from disk, and the results are written back to memory as well, such that the I/O overheads do not count into the end-to-end processing latency.

Config II. Developed upon Config I, we further use in-memory buffers to store intermediate results. Figure 3 shows that the program needs to frequently generate intermediate results between different stages and store them back into the disk, which introduces extra I/O overhead, especially when the disk bandwidth is low. This is an important step for extra-large dataset, but considering that all required data can entirely reside in the CPU’s DRAM, we use in-memory buffers to store the intermediate states instead.

Config III. Building upon Config II, we assume that the dataset is already decoded and in a ready-to-use binary format. Although most datasets are typically encoded in UTF-8, it is possible that the dataset has been previously processed and stored as a binary dataset. For the CPU baseline, we need to unpack and map binary input to be expected tuples. The overhead partially counteracts the positive impact of removing the decoding function.

Figure 8 compares the CPU performance for the three configurations, showcasing the effectiveness of our step-by-step optimizations. The two sub-figures show the performance given different vocabulary sizes of 5K and 1M, respectively. We split the whole process into four stages as illustrated in Section 2.3, including *Split Input File*, *Generate Vocab*, *Apply Vocab*, and *Concatenate*. These stages run sequentially and exhibit different scalability with multiple threads. The figure compares the performance with different numbers of threads for the same setup, neglecting the cases with few threads due to the long execution time. For all cases, Figure 8 demonstrates that the preprocessing performance does not scale linearly with the number of threads.

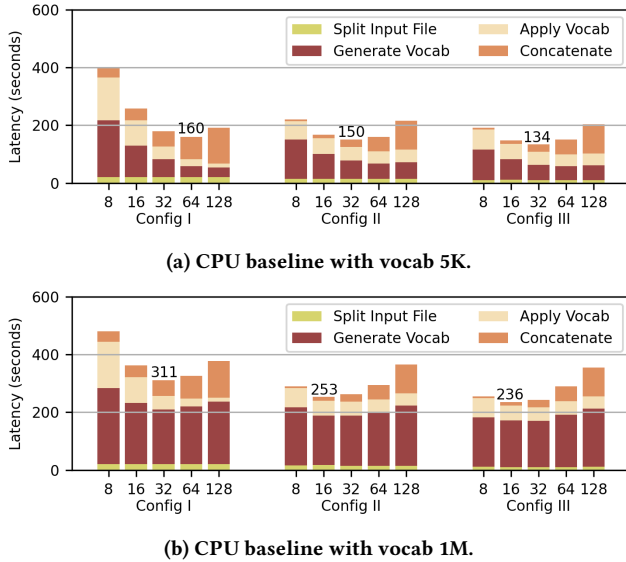


Figure 8: CPU baseline with different vocabulary sizes. The bars with numbers represents the best performance.

Figure 8a shows the performance gains of different baseline configurations given a small vocabulary size of 5K. Both Config I and II work on the UTF-8 input datasets, while Config III works on the decoded binary datasets.

For Config I that writes all intermediate results back to disk, we make several observations. Firstly, the initialization of *Split Input File* remains constant because the overhead is dominated by reading data rather than distributing it to different sub-files. Secondly, the execution time of *Generate Vocab* keeps halving until the number of threads reaches 64, with only slight improvements beyond 64 threads. Thirdly, the execution time of *Apply Vocab* continues to halve up to 128 threads. Fourthly, the execution time of *Concatenate* keeps doubling as the number of sub-files increases. This indicates that the overhead is dominated by the calls to read each sub-file rather than the reading process itself. Finally, it achieves the best performance with 64 threads.

For Config II, which allows intermediate results to be written to memory as well, we have several observations. Firstly, the initialization of *Split Input File* remains constant. Secondly, the performance of *Generate Vocab* and *Apply Vocab* saturates at 64 threads. For 64 and 128 threads, these two stages take significantly longer than in Config I, even though intermediate results are stored in DRAM. One possible reason is that a shared dictionary is introduced for row-wise multi-processing, and the synchronization overhead is significant when too many threads are involved. Thirdly, the execution time of the *Concatenate* stage doubles with the increase in threads. Compared to Config I, the cost for the same number of threads is smaller, which can be attributed to the in-memory storage of intermediate results after *Apply Vocab*. Finally, Config II achieves the best performance with 32 threads.

For Config III, which uses a decoded binary dataset as input, we make several observations. Firstly, the initialization of *Split Input File* remains constant but is much shorter than in the other two configurations. Since the input is now a binary dataset, we omit the

step of explicitly counting the number of rows with a loop; instead, we simply obtain the file size and calculate it. Secondly, the performance of *Generate Vocab* is nearly the same as in Config I. Within the reading loop, we unpack the binary input into corresponding tuples. Thirdly, the overheads for *Apply Vocab* and *Concatenate* are nearly the same as in Config I. Finally, Config III achieves the best performance with 32 threads.

Figure 8b shows that the processing latency increases given a larger vocabulary size of 1M, mainly due to the random mapping process of input features to the corresponding vocabulary. Firstly, Config I now reaches the best performance with 32 threads, while Config II and III reach the best performance with 16 threads. Secondly, for *Split Input File*, *Apply Vocab* and *Concatenate*, the performance stays the same as Vocab 5K. Thirdly, for *Generate Vocab*, the speedup of multi-threading is not prominent because the software needs to maintain a much larger dictionary to support multi-processing, and the resulting synchronization overhead also increases with the number of threads.

4.2.2 Google’s DLRM Preprocessing in Cloud. Google’s preprocessing pipeline is based on their Apache Beam implementation, which supports both local mode (Direct Runner) and distributed mode (Dataflow Runner). The direct Runner mode in the local environment only aims to validate the pipeline, and it performs poorly in our local server. The dataflow Runner works with Google Cloud. In this experiment, we only consider the execution in Google Cloud using Dataflow Runner due to its higher performance. We observe that the initialization overhead of Apache Beam pipeline is too high for both *Generate Vocab* and *Apply Vocab*. To report the best baseline performance, we measure and deduct the initialization time from the reported performance.

4.3 Preprocessing in GPU

We implement the preprocessing for DLRM in GPU with the support of Nvidia RAPIDS Suite, including *rmm*, *nvtabular*, *cudf* [56]. Its acceleration highly depends on the binary input format, like Parquet, so transforming the original dataset is a non-trivial step. The following step is to initiate a Workflow, which defines the pipeline and then finishes the preprocessing for each column independently. The top GPU utilization is over 85%.

4.4 PIPER: Performance and Efficiency

We evaluate PIPER to compare its performance with CPUs and GPUs. Specifically, we compare the end-to-end data preprocessing performance between PIPER and the optimized baselines, break down the performance for each operator, and show the performance implications of using PIPER as either a local or a networked accelerator.

Evaluation configurations. Table 2 lists the configurations we used in the comparison. For PIPER, we focus on the network-based version due to its advantages of avoiding host-side execution overhead and its ability to process datasets larger than memory. We use the local mode only to verify the functionality of the dataflow for small vocabulary sizes. For Google’s implementation, the generated binary dataset cannot be used as the input format, so we compare Google Cloud with PIPER exclusively for the UTF-8 dataset.

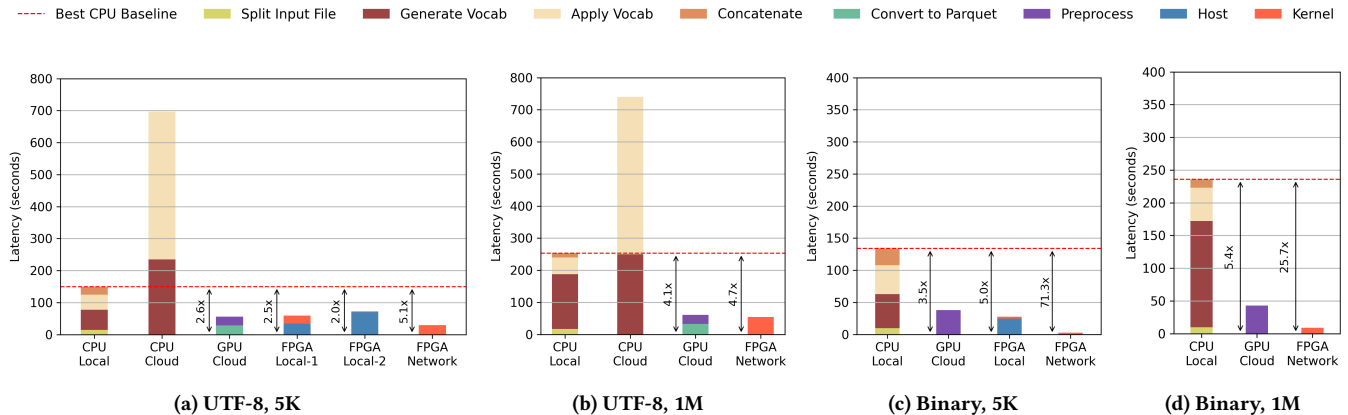


Figure 9: Performance comparison between CPU, GPU and FPGA for various configurations.

Table 2: Configurations available of CPU, GPU, and PIPER.

Vocab	Platform	UTF8	Binary
5K	CPU Local	✓	✓
	CPU Cloud	✓	×
	GPU Cloud	✓	✓
	FPGA Local	✓	✓
	FPGA Network	✓	✓
1M	CPU Local	✓	✓
	CPU Cloud	✓	×
	GPU Cloud	✓	✓
	FPGA Network	✓	✓

4.4.1 End-to-end Performance. Figure 9 compares the end-to-end preprocessing performance between the CPU, GPU and PIPER for various configurations. Figure 9a shows the performance gains of PIPER in both local and network mode for the UTF-8 dataset with a small vocabulary table. When compared with the best performance in CPU, PIPER achieves 2.5 \times and 2.0 \times speedup in local mode, respectively, depending on decoding in the kernel or the host, and achieves 5.1 \times speedup in network mode. When compared with Google Cloud, the performance gain is much higher. Figure 9b displays the acceleration of PIPER in network mode only for the UTF-8 dataset with a large vocabulary table. Here, the CPU baseline in the local machine performs better than Google Cloud, and PIPER reaches 4.7 \times speedup over the most performant CPU baseline. Figure 9c demonstrates the positive effect of using the binary dataset as input, which significantly increases the parallelism of the kernel. Specifically, the speedups of PIPER over CPUs boost to 5.0 \times and 71.3 \times respectively in local and network mode. Figure 9d further indicates the performance enhancement of PIPER in network mode for the binary dataset with a large vocabulary table, where PIPER obtains speedup by 25.7 \times .

Compared to GPU, Figure 9 shows that it also reaches 2.6~5.4 \times speedup when compared with the local CPU baseline. When the

input data format is UTF-8, PIPER achieves slightly better performance. However, when the input is binary format, the speedup of PIPER grows significantly, ranging from 4.8~20.3 \times .

4.4.2 PIPER with Decoder. For PIPER, the default input data format is UTF-8 due to its prevalence in DLRM datasets. To ensure ease of use and compatibility with this commonly used data format, we optimized the *Decode* function as described in Section 3.3 to increase the decoding throughput.

While decoding on FPGA is faster compared to the CPU version, the *Decode* implementation still limits the degree of parallelism in the PIPER dataflow. Specifically, Figure 9a shows that the acceleration ratio of PIPER can reach 2.5 \times compared to the best performance of a powerful server-level 128-core CPU, while the hybrid CPU-FPGA architecture only achieves 2.0 \times speedup over the CPU.

4.4.3 Maximizing Kernel Performance by Offloading Decoding. Maximizing the throughput of FPGA’s off-chip memory is essential to achieve the best performance of PIPER, and there are two ways to achieve it. Firstly, Figure 9a illustrates that if we relocate *Decode* in the host, the kernel execution time drops significantly. Nevertheless, the end-to-end speedup of PIPER decreases to 2.0 \times because the extra overhead in the host for decoding is significant for end-to-end execution. Secondly, Figure 9c reveals that if we use a pre-decoded binary dataset instead as the input, the speedup of PIPER in the local mode increases to 5.0 \times because the kernel execution benefits a lot from parallel PE design and the overhead in the host only involves data transmission.

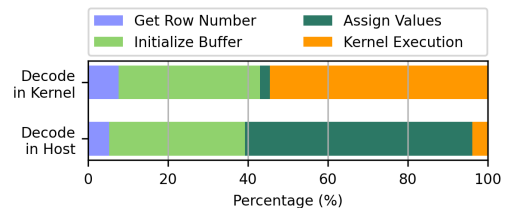


Figure 10: Time breakdown of PIPER in local mode.

4.4.4 Execution Time Breakdown. It would be ideal to understand the performance of each of the processing stages: *Get Row Number*,

Table 3: Throughput in row per second for pure computation (original & config I: UTF-8, config II: binary).

Vocab	Dataset	CPU						FPGA	
		CPU-1	CPU-8	CPU-16	CPU-32	CPU-64	CPU-128	Local	Network
5K	Config I	1.84E+4	1.32E+5	2.32E+5	4.32E+5	7.39E+5	9.75E+5	1.87E+6	1.56E+6
	Config II	4.02E+4	2.30E+5	3.27E+5	4.16E+5	4.82E+5	4.53E+5	1.87E+6	1.56E+6
	Config III	4.96E+4	2.61E+5	3.69E+5	4.67E+5	5.09E+5	4.92E+5	1.77E+7	2.36E+7
1M	Config I	1.50E+4	1.08E+5	1.52E+5	1.93E+5	2.01E+5	1.98E+5		8.45E+5
	Config II	3.81E+4	1.71E+5	2.05E+5	2.06E+5	1.99E+5	1.83E+5		8.45E+5
	Config III	4.51E+4	1.92E+5	2.15E+5	2.20E+5	2.00E+5	1.87E+5		4.99E+6

Initialize Buffer, Assign Values & Kernel Execution. To this end, we break down the time consumption per stage using PIPER as a local accelerator. Specifically, there are several aspects worth noticing during the profiling. Firstly, we need to know the number of rows of the input dataset to determine the size of the CPU’s buffer and FPGA’s off-chip memory. Secondly, the design of regarding FPGA as an attached accelerator must consider data movements. When transferring the dataset into FPGA’s memory, we can read large chunks of data to increase the efficiency. Here, the initialization overhead of creating large buffers dominates, and it can reach tens of seconds. Thirdly, for the scenario of implementing a decoding function in CPU as shown in Figure 7b, the program can only read the file per byte, and it is time-consuming; otherwise, it can simply read the file and store the content into the buffer. Finally, the execution time includes transferring data from host to kernel, kernel operations, and transferring data from kernel to host. For our case, we focus on kernel operations, and profiling tools are very helpful in generating a summary report.

Figure 10 shows the time breakdown of running PIPER in local mode, with the extra host-side overhead partially explaining why using PIPER as a local accelerator is sub-optimal for preprocessing. We focus on two modes: *Decode in Kernel* and *Decode in Host*, as shown in Figure 7b and 7c. For *Decode in Kernel*, the decoding function takes a significant amount of time in the kernel, but *Initialize Buffer* still occupies a large portion of execution time. For *Decode in Host*, where the decoding function is moved to the host, the execution takes about 50% longer than performing the decoding function twice in the kernel. In this condition, the proportion of time spent on *Initialize Buffer* remains very high.

4.4.5 PIPER with Network. When serving as a network-attached rather than a local accelerator, PIPER not only becomes more flexible in data centers but also achieves better performance as the host-side initialization overhead is removed and we then expect a fully-pipelined running fashion. Figure 9a and 9b show PIPER’s performance when acting as a network-attached accelerator. It achieves speedups of 5.1× and 4.7×, respectively, compared to the best performance of a 128-core CPU for the UTF-8 dataset. Figures

9c and 9d show that PIPER reaches speedups of 71.3× and 25.7× for the binary dataset, where PIPER maximizes its parallelism and the kernel execution time is negligible.

4.4.6 Throughput of Pure Computation. Table 3 shows the throughput for pure computation of all configurations to demonstrate the computing capability of PIPER versus multi-core CPUs. We measure the throughput without data loading and storing steps to eliminate potential data movement overheads. In the CPU setup, we exclude *Split Input File & Concatenate*, as these steps are not directly involved in the computation. To ensure the validity of results, we conducted repetitive tests to guarantee that all data comes from DRAM and used the average performance of three runs as the final result. For PIPER, we report the kernel execution time. The difference between local and network mode lies in the kernel clock frequency of the FPGA.

By eliminating the non-computing steps, Table 3 compares performance gains of PIPER for stateful preprocessing pipelines with/without raw dataset transformation. Given the UTF-8 input dataset (Config I & II) and a small vocabulary table, the CPU reaches the highest throughput in Config II with 64 threads, and PIPER achieves 4.1× speedup over CPU. Given the binary input dataset, the speedup of PIPER increase to 46.4×. When the vocabulary size increases to 1M, the performance of both CPU and PIPER decreases due to the more frequent random memory accesses. In this setup, PIPER achieves speedups of 4.2× for the UTF-8 dataset and 22.7× for the binary dataset. Given these numbers, PIPER running in networked mode is preferable for adapting to various configurations, and serving binary dataset as input can significantly increase its performance for both end-to-end execution and pure computation. The theoretical maximum throughput for binary input can be 30.2 Gbit/s for 5K vocabulary and 6.4 Gbit/s for 1M vocabulary, and using multiple FPGAs can further improve the overall performance.

Table 4 compares the performance of each individual operator between PIPER and the CPU. It shows that for some operators like *Neg2Zero*, *Logarithm*, CPU outperforms FPGA greatly; while for some other operators, especially for *Hex2Int & Modulus*, FPGA performs much better. For *ApplyVocab*, using HBM as a cache to

support a large vocabulary table results in an Π of one cycle, because independent channels are used for different features and memory access occurs in a round-robin manner. The time span for accessing the same HBM channel is longer than the allowed Π for random access. Besides, FPGA can process the task in a pipelined manner, so we only need to carefully optimize the critical operator, i.e. *GenVocab* in this case. However, on the CPU, the total execution time includes all operators, requiring each to be optimized to minimize the overall latency.

Table 4: Comparison of execution time of operators in seconds for the whole dataset in different platforms (CPU single thread; FPGA 250MHz for vocab 5K and 135MHz for vocab 1M). 7.33s and 13.58s represents $\Pi=1$ in 250MHz and 135MHz respectively.

Vocab Platform	5K		1M	
	CPU	FPGA	CPU	FPGA
Decode & FillMissing	182.29±1.10	11.00	182.29±1.10	20.37
Binary Unpack	35.77±0.57	7.33	35.77±0.57	13.58
Hex2Int & Modulus	655.17±1.55	7.33	655.17±1.55	13.58
GenVocab-1	365.34±1.59	14.67	410.82±5.34	27.16
GenVocab-2	NOP	7.33	NOP	13.58
ApplyVocab-1	0.0065±0.00024	7.33	0.74±0.015	13.58
ApplyVocab-2	331.79±1.51	7.33	367.11±9.54	13.58
Neg2Zero	0.61±0.0071	7.33	0.61±0.0071	13.58
Logarithm	1.34±0.012	7.33	1.34±0.012	13.58

5 DISCUSSION

In this section, we discuss how PIPER can be extended for various deployment and algorithm requirements.

Integration into ML systems. To integrate PIPER into the current training system, cloud vendors can add an interface between PIPER and machine learning training frameworks such as PyTorch and TensorFlow, facilitating data transfer between GPUs and FPGAs. As PIPER already supports networked execution modes, the interface can be as simple as initiating the service of sending/receiving training data over the network, like Remote Procedure Call (RPC) [18, 54]. The recently released FPGA-based smart NIC products like MangoBoost RDMA System [48] enable 200Gbps throughput, which provides a solid foundation for the communication between peripheral PCIe devices (FPGAs) and GPUs.

Generalizability for other preprocessing pipelines. In this paper, DLRM works as a representation of ML-based recommender systems where other models share a similar tabular data input and preprocessing pipeline. In order to support other data preprocessing pipelines, we build PIPER in a modular fashion, such that the operators PIPER supports can be easily integrated into alternative pipelines. Using available FPGA virtualization and multi-tenancy techniques [35, 40, 47], it is feasible to dynamically configure the operators in the pipeline at runtime.

Cater to tabular datasets. The concept of sparse and dense features works for many tabular datasets, like MovieLens [28], Netflix Prize Dataset [9], Amazon Product Review Data [27], Yelp Dataset [5]. The modular design of PIPER allows users to easily

adjust the number of dataflows to adapt to different numbers of feature columns.

6 RELATED WORK

To our knowledge, PIPER is the first attempt at addressing the efficiency of tabular data preprocessing pipelines with specialized hardware design.

Data preprocessing frameworks for CPUs. Currently, the CPU is the mainstream platform for preprocessing tasks of machine learning. Google introduced `tf.data` [52] and developed `tf.data service` [6] to strengthen disaggregated data processing service.

Preprocessing performance optimizations on CPUs. UP-LIFT [63] focuses on the parallelization of feature transformations. Plumber [42] help users find bottlenecks in ML input pipelines. Cachew [23] supports *auto-scaling* and *auto-caching* policies to minimize training time and cost. GoldMiner [81] decouples stateless data preprocessing from model training in the cloud environment. FastFlow [73] offloads input pipelines to remote CPUs, and FusionFlow [36] utilizes both CPUs and GPUs to accelerate preprocessing.

Improved DLRM training. Neo [51] proposes a SW-HW co-designed system for distributed training of large-scale DLRMs. Dhiraaj [34] optimizes DLRM training on CPU cluster architectures. EL-rec [76] harness the tensor-train technique for large-scale DLRMs with limited GPU resources. cDLRM [7] trains on a single GPU by storing all embedding tables in CPU memory. RecD [83] optimizes DLRM data generation pipelines to decrease dataset storage.

FPGA in Data Center. Microsoft’s Catapult [64] uses FPGAs to implement network virtualization in hyper-scale data centers. StRoM [67] presents a programmable, FPGA-based RoCE v2 NIC. IBM [77] proposes a cloud computing software service to integrate FPGAs in the cloud. Naif [70] create network FPGA clusters in a heterogeneous cloud data center.

7 CONCLUSION

We present PIPER, a network-based hardware accelerator to support tabular stateful data preprocessing for embedding generation. To address the computationally intensive data preprocessing workload, PIPER incorporates high-performance data transformation units and various operator processing units. For flexible integration into end-to-end machine learning training systems, PIPER can function both as a local accelerator and as a network-attached accelerator. PIPER achieves 4.7~71.3× speedup over a 128-core CPU server and 4.8~20.3× over a data-center GPU. This impressive performance highlights PIPER’s potential for future integration into production ML training systems.

REFERENCES

- [1] Josh Achiam, Steven Adler, Sandhini Agarwal, Lama Ahmad, Ilge Akkaya, Florencia Leoni Aleman, Diogo Almeida, Janko Alentschmidt, Sam Altman, Shyamal Anadkat, et al. 2023. Gpt-4 technical report. *arXiv preprint arXiv:2303.08774* (2023).
- [2] Catalina Alvarez, Zhenhao He, Gustavo Alonso, and Ankit Singla. 2020. Specializing the network for scatter-gather workloads. In *Proceedings of the 11th ACM Symposium on Cloud Computing*. 267–280.
- [3] Amazon. 2024. AQUA (Advanced Query Accelerator) – A Speed Boost for Your Amazon Redshift Queries. <https://aws.amazon.com/blogs/aws/new-aqua-advanced-query-accelerator-for-amazon-redshift>
- [4] Sebastian Angel, Mihir Nanavati, and Siddhartha Sen. 2020. Disaggregation and the Application. In *12th USENIX Workshop on Hot Topics in Cloud Computing (HotCloud 20)*.

- [5] Nabih Asghar. 2016. Yelp dataset challenge: Review rating prediction. *arXiv preprint arXiv:1605.05362* (2016).
- [6] Andrew Audibert, Yang Chen, Dan Graur, Ana Klimovic, Jiří Šimša, and A Chandramohan. 2023. tf.data service: A Case for Disaggregating ML Input Data Processing. (2023).
- [7] Keshav Balasubramanian, Abdulla Alshabanah, Joshua D Choe, and Murali Annaram. 2021. cDLRM: Look ahead caching for scalable training of recommendation models. In *Proceedings of the 15th ACM Conference on Recommender Systems*. 263–272.
- [8] Matěj Bartík, Sven Ubik, and Pavel Kubalik. 2015. LZ4 compression algorithm on FPGA. In *2015 IEEE International Conference on Electronics, Circuits, and Systems (ICECS)*. IEEE, 179–182.
- [9] James Bennett, Stan Lanning, et al. 2007. The netflix prize. In *Proceedings of KDD cup and workshop*, Vol. 2007. New York, 35.
- [10] Marco Spaziani Brunella, Giacomo Belocchi, Marco Bonola, Salvatore Pontarelli, Giuseppe Siracusano, Giuseppe Bianchi, Aniello Cammarano, Alessandro Palumbo, Luca Petrucci, and Roberto Bifulco. 2022. hXDP: Efficient software packet processing on FPGA NICs. *Commun. ACM* 65, 8 (2022), 92–100.
- [11] Heng-Tze Cheng, Levent Koc, Jeremiah Harmsen, Tal Shaked, Tushar Chandra, Hrish Aradhye, Glen Anderson, Greg Corrado, Wei Chai, Mustafa Ispir, et al. 2016. Wide & deep learning for recommender systems. In *Proceedings of the 1st workshop on deep learning for recommender systems*. 7–10.
- [12] Jack Choquette. 2023. Nvidia hopper h100 gpu: Scaling performance. (2023).
- [13] Kenneth Ward Church. 2017. Word2Vec. *Natural Language Engineering* 23, 1 (2017), 155–162.
- [14] Criteo. 2024. Criteo Kaggle Dataset. <https://www.kaggle.com/datasets/mrkmakr/criteo-dataset>
- [15] William J Dally, Stephen W Keckler, and David B Kirk. 2021. Evolution of the graphics processing unit (GPU). *IEEE Micro* 41, 6 (2021), 42–51.
- [16] Tudor David, Rachid Guerraoui, and Vasileios Trigonakis. 2013. Everything you always wanted to know about synchronization but were afraid to ask. In *Proceedings of the Twenty-Fourth ACM Symposium on Operating Systems Principles*. 33–48.
- [17] Jacob Devlin. 2018. Bert: Pre-training of deep bidirectional transformers for language understanding. *arXiv preprint arXiv:1810.04805* (2018).
- [18] Erik H D'Hollander, Bruno Chevalier, and Koen De Bosschere. 2017. Calling hardware procedures in a reconfigurable accelerator using RPC-FPGA. In *2017 International Conference on Field Programmable Technology (ICFPT)*. IEEE, 271–274.
- [19] Haggai Eran, Lior Zeno, Maroun Tork, Gabi Malka, and Mark Silberstein. 2019. {NICA}: An infrastructure for inline acceleration of network applications. In *2019 USENIX Annual Technical Conference (USENIX ATC 19)*. 345–362.
- [20] Panagiota Fatourou and Nikolaos D Kallimanis. 2012. Revisiting the combining synchronization technique. In *Proceedings of the 17th ACM SIGPLAN symposium on Principles and Practice of Parallel Programming*. 257–266.
- [21] Daniel Firestone, Andrew Putnam, Sambhrama Mundkur, Derek Chiou, Alireza Dabagh, Mike Andrewartha, Hari Angepat, Vivek Bhanu, Adrian Caulfield, Eric Chung, et al. 2018. Azure accelerated networking: Smartnics in the public cloud. In *15th {USENIX} Symposium on Networked Systems Design and Implementation ({NSDI} 18)*. 51–66.
- [22] Google. 2024. Google Tensorflow TFRecord. https://www.tensorflow.org/tutorials/load_data/tfrecord
- [23] Dan Graur, Damien Aymon, Dan Kluser, Tanguy Albrici, Chandramohan A Thekkath, and Ana Klimovic. 2022. Cachew: Machine learning input data processing as a service. In *2022 USENIX Annual Technical Conference (USENIX ATC 22)*. 689–706.
- [24] Alex Graves and Alex Graves. 2012. Long short-term memory. *Supervised sequence labelling with recurrent neural networks* (2012), 37–45.
- [25] Udit Gupta, Samuel Hsia, Vikram Saraph, Xiaodong Wang, Brandon Reagen, Gu-Yeon Wei, Hsien-Hsin S Lee, David Brooks, and Carole-Jean Wu. 2020. Deeprecsys: A system for optimizing end-to-end at-scale neural recommendation inference. In *2020 ACM/IEEE 47th Annual International Symposium on Computer Architecture (ISCA)*. IEEE, 982–995.
- [26] Udit Gupta, Carole-Jean Wu, Xiaodong Wang, Maxim Naumov, Brandon Reagen, David Brooks, Bradford Cottel, Kim Hazelwood, Mark Hempstead, Bill Jia, et al. 2020. The architectural implications of facebook's dnn-based personalized recommendation. In *2020 IEEE International Symposium on High Performance Computer Architecture (HPCA)*. IEEE, 488–501.
- [27] Tanjim Ul Haque, Nudrat Nawal Saber, and Faisal Muhammad Shah. 2018. Sentiment analysis on large scale Amazon product reviews. In *2018 IEEE international conference on innovative research and development (ICIRD)*. IEEE, 1–6.
- [28] F Maxwell Harper and Joseph A Konstan. 2015. The movielens datasets: History and context. *Acm transactions on interactive intelligent systems (tiis)* 5, 4 (2015), 1–19.
- [29] Xiangnan He, Lizi Liao, Hanwang Zhang, Liqiang Nie, Xia Hu, and Tat-Seng Chua. 2017. Neural collaborative filtering. In *Proceedings of the 26th international conference on world wide web*. 173–182.
- [30] Zhenhao He, Dario Korolija, Yu Zhu, Benjamin Ramhorst, Tristan Laan, Lucian Petrica, Michaela Blott, and Gustavo Alonso. 2023. ACCL+: an FPGA-Based Collective Engine for Distributed Applications. *arXiv preprint arXiv:2312.11742* (2023).
- [31] Danny Hendler, Itai Incze, Nir Shavit, and Moran Tzafrir. 2010. Flat combining and the synchronization-parallelism tradeoff. In *Proceedings of the twenty-second annual ACM symposium on Parallelism in algorithms and architectures*. 355–364.
- [32] Maurice Herlihy, Nir Shavit, Victor Luchangco, and Michael Spear. 2020. *The art of multiprocessor programming*. Newnes.
- [33] Wenqi Jiang, Zhenhao He, Shuai Zhang, Kai Zeng, Liang Feng, Jiansong Zhang, Tongxuan Liu, Yong Li, Jingren Zhou, Ce Zhang, et al. 2021. Fleetrec: Large-scale recommendation inference on hybrid gpu-fpga clusters. In *Proceedings of the 27th ACM SIGKDD Conference on Knowledge Discovery & Data Mining*. 3097–3105.
- [34] Dhiraj Kalamkar, Evangelos Georganas, Sudarshan Srinivasan, Jianping Chen, Mikhail Shiryaev, and Alexander Heinecke. 2020. Optimizing deep learning recommender systems training on cpu cluster architectures. In *SC20: International Conference for High Performance Computing, Networking, Storage and Analysis*. IEEE, 1–15.
- [35] Ahmed Khawaja, Joshua Landgraf, Rohith Prakash, Michael Wei, Eric Schkufza, and Christopher J Rossbach. 2018. Sharing, Protection, and Compatibility for Reconfigurable Fabric with {AmorphOS}. In *13th USENIX Symposium on Operating Systems Design and Implementation (OSDI 18)*. 107–127.
- [36] Taeyoon Kim, ChanHo Park, Mansur Mukimbekov, Heelim Hong, Minseok Kim, Ze Jin, Kangdae Kim, Ji-Yong Shin, and Myeongjae Jeon. 2023. FusionFlow: Accelerating Data Preprocessing for Machine Learning with CPU-GPU Cooperation. *Proceedings of the VLDB Endowment* 17, 4 (2023), 863–876.
- [37] Diederik P Kingma. 2013. Auto-encoding variational bayes. *arXiv preprint arXiv:1312.6114* (2013).
- [38] Ana Klimovic, Christos Kozyrakis, Eno Thereska, Binu John, and Sanjeev Kumar. 2016. Flash storage disaggregation. In *Proceedings of the Eleventh European Conference on Computer Systems*. 1–15.
- [39] Dario Korolija, Dimitrios Koutsoukos, Kimberly Keeton, Konstantin Taranov, Dejan Milojičić, and Gustavo Alonso. 2021. Farview: Disaggregated memory with operator off-loading for database engines. *arXiv preprint arXiv:2106.07102* (2021).
- [40] Dario Korolija, Timothy Roscoe, and Gustavo Alonso. 2020. Do {OS} abstractions make sense on {FPGAs}? In *14th USENIX Symposium on Operating Systems Design and Implementation (OSDI 20)*. 991–1010.
- [41] Atsushi Koshihara, Felix Gust, Julian Pritzi, Anjo Vahldiek-Oberwagner, Nuno Santos, and Pramod Bhatotia. 2023. Trusted Heterogeneous Disaggregated Architectures. In *Proceedings of the 14th ACM SIGOPS Asia-Pacific Workshop on Systems*. 72–79.
- [42] Michael Kuchnik, Ana Klimovic, Jiri Simsa, Virginia Smith, and George Amvrosiadis. 2022. Plumber: Diagnosing and removing performance bottlenecks in machine learning data pipelines. *Proceedings of Machine Learning and Systems* 4 (2022), 33–51.
- [43] Nikita Lazarev, Neil Adit, Shaojie Xiang, Zhiru Zhang, and Christina Delimitrou. 2020. Dagger: Towards efficient rpcs in cloud microservices with near-memory reconfigurable nics. *IEEE Computer Architecture Letters* 19, 2 (2020), 134–138.
- [44] Morgan Ledwon, Bruce F Cockburn, and Jie Han. 2020. High-throughput FPGA-based hardware accelerators for deflate compression and decompression using high-level synthesis. *IEEE Access* 8 (2020), 62207–62217.
- [45] Feifei Li. 2019. Cloud-native database systems at Alibaba: Opportunities and challenges. *Proceedings of the VLDB Endowment* 12, 12 (2019), 2263–2272.
- [46] Xiufeng Liu, Christian Thomsen, and Torben Bach Pedersen. 2012. MapReduce-Based Dimensional ETL Made Easy. *Proc. VLDB Endow.* 5, 12 (2012).
- [47] Jiacheng Ma, Gefei Zuo, Kevin Loughlin, Xiaohu Cheng, Yanqiang Liu, Abel Mu-lugeta Eneyew, Zhengwei Qi, and Baris Kasikci. 2020. A hypervisor for shared-memory FPGA platforms. In *Proceedings of the Twenty-Fifth International Conference on Architectural Support for Programming Languages and Operating Systems*. 827–844.
- [48] MangoBoost. 2024. MangoBoost GPU over RDMA System. <https://www.mangoboost.io/products/gpu-over-rdma#fastFact>
- [49] Larry R Medsker, Lakhmi Jain, et al. 2001. Recurrent neural networks. *Design and Applications* 5, 64-67 (2001), 2.
- [50] Meta. 2024. Meta's DLRM Preprocessing Pipeline. <https://github.com/facebookresearch/dlrm>
- [51] Dheevatsa Mudigere, Yuchen Hao, Jianyu Huang, Zhihao Jia, Andrew Tulloch, Srinivas Sridharan, Xing Liu, Mustafa Ozdal, Jade Nie, Jongsoo Park, et al. 2022. Software-hardware co-design for fast and scalable training of deep learning recommendation models. In *Proceedings of the 49th Annual International Symposium on Computer Architecture*. 993–1011.
- [52] Derek G Murray, Jiri Simsa, Ana Klimovic, and Ihor Indyk. 2021. tf.data: A machine learning data processing framework. *arXiv preprint arXiv:2101.12127* (2021).
- [53] Maxim Naumov, Dheevatsa Mudigere, Hao-Jun Michael Shi, Jianyu Huang, Narayanan Sundaraman, Jongsoo Park, Xiaodong Wang, Udit Gupta, Carole-Jean Wu, Alison G Azzolini, et al. 2019. Deep learning recommendation model

- for personalization and recommendation systems. *arXiv preprint arXiv:1906.00091* (2019).
- [54] Bruce Jay Nelson. 1981. *Remote procedure call*. Carnegie Mellon University.
- [55] Nvidia. 2024. Nvidia Data Loading Library. <https://github.com/NVIDIA/DALI/tree/main/dali/pipeline>
- [56] Nvidia. 2024. Nvidia DLRM Example. <https://github.com/NVIDIA/DeepLearningExamples/tree/master/PyTorch/Recommendation/DLRM>
- [57] Nvidia. 2024. Nvidia DLRM Optimization. <https://developer.nvidia.com/blog/optimizing-dlrm-on-nvidia-gpus/>
- [58] Nvidia. 2024. Nvidia Rapids. <https://developer.nvidia.com/rapids>
- [59] Johan Peltenburg, Lars TJ Van Leeuwen, Joost Hoozemans, Jian Fang, Zaid Al-Ars, and H Peter Hofstee. 2020. Battling the CPU bottleneck in apache parquet to arrow conversion using FPGA. In *2020 international conference on Field-Programmable technology (ICFPT)*. IEEE, 281–286.
- [60] Johan Peltenburg, Jeroen Van Straten, Lars Wijtemans, Lars Van Leeuwen, Zaid Al-Ars, and Peter Hofstee. 2019. Fletcher: A framework to efficiently integrate FPGA accelerators with apache arrow. In *2019 29th International Conference on Field Programmable Logic and Applications (FPL)*. IEEE, 270–277.
- [61] Ivy Peng, Roger Pearce, and Maya Gokhale. 2020. On the memory underutilization: Exploring disaggregated memory on hpc systems. In *2020 IEEE 32nd International Symposium on Computer Architecture and High Performance Computing (SBAC-PAD)*. IEEE, 183–190.
- [62] Jeffrey Pennington, Richard Socher, and Christopher D Manning. 2014. Glove: Global vectors for word representation. In *Proceedings of the 2014 conference on empirical methods in natural language processing (EMNLP)*. 1532–1543.
- [63] Arnab Phani, Lukas Erlbacher, and Matthias Boehm. 2022. UPLIFT: parallelization strategies for feature transformations in machine learning workloads. *Proceedings of the VLDB Endowment* 15, 11 (2022), 2929–2938.
- [64] Andrew Putnam. 2017. FPGAs in the datacenter: Combining the worlds of hardware and software development. In *Proceedings of the on Great Lakes Symposium on VLSI 2017*. 5–5.
- [65] Vijayshankar Raman and Joseph M. Hellerstein. 2001. Potter’s Wheel: An Interactive Data Cleaning System. In *Proceedings of the 27th International Conference on Very Large Data Bases (VLDB ’01)*.
- [66] Suzanne Rigler, William Bishop, and Andrew Kennings. 2007. FPGA-based lossless data compression using Huffman and LZ77 algorithms. In *2007 Canadian conference on electrical and computer engineering*. IEEE, 1235–1238.
- [67] David Sidler, Zeke Wang, Monica Chiosa, Amit Kulkarni, and Gustavo Alonso. 2020. StRoM: smart remote memory. In *Proceedings of the Fifteenth European Conference on Computer Systems*. 1–16.
- [68] Fei Sun, Jun Liu, Jian Wu, Changhua Pei, Xiao Lin, Wenwu Ou, and Peng Jiang. 2019. BERT4Rec: Sequential recommendation with bidirectional encoder representations from transformer. In *Proceedings of the 28th ACM international conference on information and knowledge management*. 1441–1450.
- [69] Yutian Sun, Tim Meehan, Rebecca Schlussel, Wenlei Xie, Masha Basmanova, Orri Erling, Andrii Rosa, Shixuan Fan, Rongrong Zhong, Arun Thirupathi, Nikhil Collooru, Ke Wang, Sameer Agarwal, Arjun Gupta, Dionysios Logothetis, Kostas Xirogiannopoulos, Amit Dutta, Varun Gajjala, Rohit Jain, Ajay Palakuzhy, Prithvi Pandian, Sergey Pershin, Abhisek Saikia, Pranjal Shankhdhar, Neerad Somanchi, Swapnil Tailor, Jialiang Tan, Sreeni Viswanadha, Zac Wen, Biswapesh Chattopadhyay, Bin Fan, Deepak Majeti, and Aditi Pandit. 2023. Presto: A Decade of SQL Analytics at Meta. *Proceedings of the ACM Conference on Management of Data (SIGMOD)* 1, 2 (jun 2023).
- [70] Naif Tarafdar, Thomas Lin, Eric Fukuda, Hadi Bannazadeh, Alberto Leon-Garcia, and Paul Chow. 2017. Enabling flexible network FPGA clusters in a heterogeneous cloud data center. In *Proceedings of the 2017 ACM/SIGDA International Symposium on Field-Programmable Gate Arrays*. 237–246.
- [71] Tensorflow. 2024. Tensorflow DLRM. <https://github.com/tensorflow/models/tree/master/official/recommendation/ranking>
- [72] Yuta Tokusashi, Huynh Tu Dang, Fernando Pedone, Robert Soulé, and Noa Zilberman. 2019. The case for in-network computing on demand. In *Proceedings of the Fourteenth EuroSys Conference 2019*. 1–16.
- [73] Taegeon Um, Byungsoo Oh, Byeongchan Seo, Minhyeok Kweun, Goeun Kim, and Woo-Yeon Lee. 2023. Fastflow: Accelerating deep learning model training with smart offloading of input data pipeline. *Proceedings of the VLDB Endowment* 16, 5 (2023), 1086–1099.
- [74] Deepak Vohra and Deepak Vohra. 2016. Apache parquet. *Practical Hadoop Ecosystem: A Definitive Guide to Hadoop-Related Frameworks and Tools* (2016), 325–335.
- [75] Zeke Wang, Hongjing Huang, Jie Zhang, Fei Wu, and Gustavo Alonso. 2022. FpgaNIC: An FPGA-based Versatile 100Gb SmartNIC for GPUs. In *2022 USENIX Annual Technical Conference (ATC)*.
- [76] Zheng Wang, Yuke Wang, Boyuan Feng, Dheevatsa Mudigere, Bharath Muthiah, and Yufei Ding. 2022. EL-rec: Efficient large-scale recommendation model training via tensor-train embedding table. In *SC22: International Conference for High Performance Computing, Networking, Storage and Analysis*. IEEE, 1–14.
- [77] Jagath Weerasinghe, Francois Abel, Christoph Hagleitner, and Andreas Herkersdorf. 2015. Enabling FPGAs in hyperscale data centers. In *2015 IEEE 12th Intl Conf on Ubiquitous Intelligence and Computing and 2015 IEEE 12th Intl Conf on Autonomic and Trusted Computing and 2015 IEEE 15th Intl Conf on Scalable Computing and Communications and Its Associated Workshops (UIC-ATC-ScalCom)*. IEEE, 1078–1086.
- [78] Ying Yang, Niccolò Meneghetti, Ronny Fehling, Zhen Hua Liu, and Oliver Kennedy. 2015. Lenses: An on-Demand Approach to ETL. *Proc. VLDB Endow.* 8, 12 (aug 2015), 1578–1589.
- [79] Qizhen Zhang, Yifan Cai, Xinyi Chen, Sebastian Angel, Ang Chen, Vincent Liu, and Boon Thau Loo. 2020. Understanding the effect of data center resource disaggregation on production dbms. *Proceedings of the VLDB Endowment* 13, 9 (2020).
- [80] Teng Zhang, Jianying Wang, Xuntao Cheng, Hao Xu, Nanlong Yu, Gui Huang, Tieying Zhang, Dengcheng He, Feifei Li, Wei Cao, et al. 2020. {FPGA-Accelerated} Compactions for {LSM-based} {Key-Value} Store. In *18th USENIX Conference on File and Storage Technologies (FAST 20)*. 225–237.
- [81] Hanyu Zhao, Zhi Yang, Yu Cheng, Chao Tian, Shiru Ren, Wencong Xiao, Man Yuan, Langshi Chen, Kaibo Liu, Yang Zhang, et al. 2023. GoldMiner: Elastic Scaling of Training Data Pre-Processing Pipelines for Deep Learning. *Proceedings of the ACM on Management of Data* 1, 2 (2023), 1–25.
- [82] Mark Zhao, Niket Agarwal, Aarti Basant, Buğra Gedik, Satadru Pan, Mustafa Ozdal, Rakesh Komuravelli, Jerry Pan, Tianshu Bao, Haowei Lu, et al. 2022. Understanding data storage and ingestion for large-scale deep recommendation model training: Industrial product. In *Proceedings of the 49th Annual International Symposium on Computer Architecture*. 1042–1057.
- [83] Mark Zhao, Dhruv Choudhary, Devashish Tyagi, Ajay Somani, Max Kaplan, Sung-Han Lin, Sarunya Pumma, Jongsoo Park, Aarti Basant, Niket Agarwal, et al. 2023. RecD: Deduplication for end-to-end deep learning recommendation model training infrastructure. *Proceedings of Machine Learning and Systems* 5 (2023).
- [84] Zhe Zhao, Lichan Hong, Li Wei, Jilin Chen, Aniruddh Nath, Shawn Andrews, Aditee Kumathekar, Maheswaran Sathiamoorthy, Xinyang Yi, and Ed Chi. 2019. Recommending what video to watch next: a multitask ranking system. In *Proceedings of the 13th ACM Conference on Recommender Systems*. 43–51.
- [85] Guorui Zhou, Xiaoqiang Zhu, Chenru Song, Ying Fan, Han Zhu, Xiao Ma, Yanghui Yan, Junqi Jin, Han Li, and Kun Gai. 2018. Deep interest network for click-through rate prediction. In *Proceedings of the 24th ACM SIGKDD international conference on knowledge discovery & data mining*. 1059–1068.
- [86] Yue Zhu, Weikuan Yu, Bing Jiao, Kathryn Mohror, Adam Moody, and Fahim Chowdhury. 2019. Efficient user-level storage disaggregation for deep learning. In *2019 IEEE International Conference on Cluster Computing (CLUSTER)*. IEEE, 1–12.